Li *et al. Cell Communication and Signaling* (2025) 23:230
https://doi.org/10.1186/s12964-025-02236-6

Cell Communication and Signaling

RESEARCH Open Access

Prkci promotes colorectal cancer metastasis by phosphorylating and stabilizing Tgfbr1 to activate TGF-β signaling

Peng Li[1*], Guangshi Liu[1], Wenbin Zhang[2] and Tao Li[1]

Abstract

Colorectal cancer is one of the most common malignancies worldwide, with metastasis being the leading cause of cancer-related mortality. However, the molecular mechanisms driving CRC metastasis remain poorly understood. In this study, we identified Prkci as a critical oncogenic driver in CRC metastasis. Prkci was significantly upregulated in metastatic CRC tissues. Mechanistically, Prkci phosphorylated and stabilized Tgfbr1, a key receptor in the Transforming Growth Factor Beta signaling pathway, preventing its proteasomal degradation and amplifying downstream signaling cascades. This stabilization promoted epithelial-to-mesenchymal transition, enhancing migratory and invasive capacities of CRC cells. In vivo, Prkci knockout significantly reduced liver and lung metastases and prolonged survival in mouse models, highlighting its therapeutic potential. These findings establish Prkci as a promising therapeutic target for suppressing CRC metastasis and improving outcomes for metastatic CRC patients.

Keywords Colorectal cancer, Prkci, TGF-β signaling, Metastasis, Tgfbr1

Background

Colorectal cancer (CRC) is the third most diagnosed cancer and a leading cause of cancer-related deaths worldwide, accounting for significant global health burdens. While advancements in early detection and treatment have improved survival rates, the prognosis for metastatic CRC (mCRC), particularly those with liver and lung metastases, remains poor, with five-year survival rates below 15% [1–4]. This underscores the critical need to better understand the molecular mechanisms underlying CRC metastasis to develop effective therapeutic strategies.

The metastasis of CRC involves a complex interplay of cellular processes, with epithelial-to-mesenchymal transition (EMT) emerging as a pivotal driver of tumor progression, invasion, and therapeutic resistance [5]. EMT is characterized by the loss of epithelial characteristics and acquisition of mesenchymal traits, which confer increased migratory and invasive capacities to cancer cells [6]. Transforming Growth Factor Beta (TGF-β) signaling is a major inducer of EMT. Aberrations in TGF-β signaling, including overexpression of key receptors like Tgfbr1 and activation of downstream Smad pathways, have been closely linked to CRC metastasis [7–9]. Inhibiting the abnormal activation of the TGF-β signaling pathway may be an effective strategy to suppress colorectal cancer metastasis [10, 11].

*Correspondence:
Peng Li
lp20014@163.com
[1]Gastrointestinal Surgery department, People Hospital of Xinjiang Uygur Autonomous Region, Xinjiang, Urumqi 830000, China
[2]Department of Gastrointestinal Surgery, Affiliated Tumor Hospital of Xinjiang Medical University, Urumqi 830001, China

Protein kinase C iota (Prkci) is an atypical serine/threonine protein kinase that plays a significant role in the development and progression of various malignancies. Studies have shown that Prkci is overexpressed in multiple cancers, including osteosarcoma, pancreatic cancer, and cervical cancer, and its high expression is closely associated with enhanced proliferation, invasion, metastasis of tumor cells, and poor prognosis in patients, For instance, in osteosarcoma, Prkci regulates the Akt/mTOR pathway to enhance tumor cell proliferation and metastasis; in pancreatic cancer, it synergizes with RIPK2 to potentiate multiple signaling pathways, driving tumor aggressiveness and liver metastasis; and in cervical cancer, Prkci reduces radiosensitivity by modulating the Hedgehog/GLI1 pathway [12–23]. These features position Prkci as a promising therapeutic target, where its inhibition could effectively curb malignant progression and enhance the efficacy of existing cancer treatments. However, the role of Prkci in colorectal cancer metastasis remains unexplored. Elucidating its function in colorectal cancer metastasis may provide insights for improving the prognosis of patients with metastatic colorectal cancer.

Here, we revealed that Prkci was significantly upregulated in metastatic CRC tissues compared to primary tumors, suggesting a pivotal role in promoting metastatic dissemination. Mechanistically, we demonstrated that Prkci phosphorylated and stabilized Tgfbr1, a key receptor in the TGF-β signaling pathway. Phosphorylated Tgfbr1 stabilization prevented its proteasomal degradation. Both in vitro and in vivo models confirmed that Prkci promoted the migratory and invasive capacities of CRC cells, while its inhibition significantly reduced metastasis to vital organs such as the liver and lungs. These findings positioned Prkci as a promising therapeutic target for suppressing CRC metastasis and improving clinical outcomes for mCRC patients.

Methods

Cell lines and culture

SW48 and LoVo cell lines were purchased from American Type Culture Collection. LoVo cells were cultured with F-12 K Medium, while SW48 cells were bought from L-15 Medium. All mediums were added with fetal bovine serum to a final concentration of 10%. Cells were maintained at 37 °C in 95% Air, 5% CO2 (LoVo) or 100% Air (SW48).

Cell lines construction

For Prkci knock-out cell lines, sgRNA-Prkci was cloned into pSpCas9(BB)-2 A-Puro (PX459) V2.0 (62988, Addgene) and transfected into cells. After transfection, the cells were selected with puromycin (2 μg/ml) for one week, followed by single-clone culture. Gene sequencing and Western blot analysis were performed to determine whether the KO cell line was successfully established. For the construction of the Prkci overexpression cell line, cDNA-Prkci was cloned into pLKO_AS3w. The lentivirus was produced using the three-plasmid packaging system consisting of MD2-G, PAX, and pLKO-AS3W. The generated lentivirus was used to infect tumor cells, and after three days, puromycin (2 μg/ml) selection was applied until all control cells were eliminated. qPCR and Western blot analysis were performed to confirm the successful establishment of the overexpression cell line. For the construction of the knockdown cell line, the three-plasmid packaging system consisting of MD2-G, PAX, and pLKO.1 was used. The subsequent procedures were similar with those used for the overexpression cell line. The sequences of sgRNA-Prkci: 5-TTAAATTATCTTCATGAGCG-3; 5-TAAATTATCTTCATGAGCGA-3; 5-CACTGACTACGGCATGTGTA-3; sgRNA-Tgfbr1: 5-TGGCAGAAACACTGTAACGC-3; 5-AATTGTCTTTTGTACAGAGG-3; 5-TAAAATTGTCTTTTGTACAG-3; shTgfbr1: 5- CACAACAGCATGTGTATAGCT-3; 5- AATGTTGGTATGCCAATGGA-3; 5- CAGTAAGTGCCACTTCTGTGT-3;

Construction of point mutant plasmid

The point mutant plasmids were constructed using Mut Express MultiS Fast Mutagenesis Kit V2 (C215, Vazyme).

Antibodies and reagents

Antibodies for Prkci (66493, proteintech), β-actin (ab8226, abcam), pan Phospho-Serine/Threonine (AP1475, Abclonal), HA-tag (66006, proteintech), His-tag (66005, proteintech), Flag-tag (66008, proteintech), Tgfbr1 (30117, proteintech), Tgfbr2 (66636, proteintech), p-Smad2 (80427, proteintech), Smad2 (67343, proteintech), p-Smad3 (ab63403, Abcam), Anti-Ubiquitin K11 linkage Antibody (2A3/2E6, sigma), Smad3 (ab208182, Abcam), and Smad4 (ab40759, Abcam) were bought from identified companies. PF-06952229 (HY-136244) was bought from MedChemExpress company.

Immunohistochemistry (IHC)

After deparaffinization and rehydration, antigen retrieval was performed, and nonspecific binding was blocked with a blocking solution. The sections were incubated with the primary antibody overnight, followed by secondary antibody incubation at room temperature. The color reaction was developed, sections were counterstained with hematoxylin, dehydrated, and mounted. Finally, the results were observed and analyzed under a microscope. Immunohistochemistry scoring was performed by selecting representative fields under a microscope, scoring staining intensity (0 for no staining, 1 for weak, 2 for moderate, and 3 for strong), and evaluating the percentage of positive cells (0 for none, 1 for ≤ 10%, 2

for 11-50%, 3 for 51-80%, and 4 for > 80%). The total score (0–12) was calculated by multiplying the two scores, and results were classified into low (0–7) or high [8–12] categories based on the total score.

Immunoblotting (IB) and immunoprecipitation (IP)

For immunoblotting, proteins were extracted, quantified, denatured, and separated by SDS-PAGE, followed by transfer to a PVDF membrane (162–0177, Bio-Rad). After blocking, the membrane was incubated with primary and secondary antibodies, and target proteins were detected using chemiluminescence. For immunoprecipitation, protein lysates were incubated with a target-specific antibody and Protein A/G beads (HY-K0202, MCE), followed by washing and elution. The eluted proteins were analyzed by immunoblotting to confirm the presence of the target protein.

Trans-well assay

In a trans-well assay, cells were suspended in serum-free medium and seeded into the upper chamber of a trans-well insert (3422, Corning), while the lower chamber contained complete medium. For invasion assays, the insert was pre-coated with Matrigel (356230, Corning). After incubation at 37 °C for 12–16 h, non-migrated cells were removed from the upper surface, and migrated cells on the lower surface were fixed, stained, and visualized under a microscope for quantification.

Wound healing assay

In a wound healing assay, cells were grown to confluence in a 6-well plate, and a straight scratch was made in the monolayer using a sterile pipette tip. Detached cells were washed away with PBS. Serum-free medium and 5-fluouracil (HY-90006, MCE) were added to minimize cell proliferation. The plate was incubated at 37 °C, and images of the wound were captured at 0 h and subsequent time points. The wound area was measured over time to evaluate cell migration rates.

Flow cytometry

Incubate Tgfbr1 WT, T47A, and T47E cells with Tgfbr1 antibody at room temperature for 2 h, followed by incubation with FITC-conjugated secondary antibody at room temperature for another 2 h. Then, analyze the FITC fluorescence intensity of the cells using flow cytometry.

Real-time PCR

Total RNA was extracted from cells or tissues, and its concentration and purity were measured. RNA was reverse transcribed into cDNA using reverse transcriptase. The reaction mix (RK21203, ABclonal), including cDNA, SYBR Green, and specific primers, was subjected to real-time PCR with fluorescence detection. The followed primers were listed as followed: Prkci F: 5-AGGTCCGGGTGAAAGCCTA-3, Prkci R: 5-TGAAGAGCTGTTCGTTGTCAAA-3; Snail F: 5- TCGGAAGCCTAACTACAGCGA-3, Snail R: 5-AGATGAGCATTGGCAGCGAG-3; Vimentin F: 5-GACGCCATCAACACCGAGTT-3, Vimentin R: 5- CTTTGTCGTTGGTTAGCTGGT-3; N-cad F: 5-TCAGGCGTCTGTAGAGGCTT-3, N-cad R: 5-ATGCACATCCTTCGATAAGACTG-3; ZO-1 F: 5- CAACATACAGTGACGCTTCACA-3, ZO-1 R: 5- CACTATTGACGTTTCCCCACTC-3; E-cad F: 5-CGAGAGCTACACGTTCACGG-3, E-cad R: 5-GGGTGTCGAGGGAAAAATAGG-3.

Mice experiment assays

Cancer cells were cultured and harvested at 70–80% confluence. A single-cell suspension was prepared in sterile PBS at a concentration of $1–4 \times 10^6$ cells/mL. For the lung metastasis model, cells in 100 µL of PBS were injected into the lateral tail vein of 8-week-old BALB/c nude mice (GemPharmatech). Mice were monitored daily for signs of distress or weight loss. For the liver metastasis model, cells in 100 µL of PBS were injected into the spleen of mice under anesthesia. To prevent further tumor dissemination from the spleen, a splenectomy was performed immediately following the injection. Mice were monitored postoperatively for recovery and disease progression. At the experimental endpoint, mice were euthanized via CO2 inhalation. Lungs and livers were harvested, rinsed in PBS, and fixed in 4% neutral buffered formalin for histological analysis. Metastatic nodules were quantified macroscopically, and tissues were embedded in paraffin for further examination using hematoxylin and eosin staining.

Statistical analysis

All single cell sequencing databases and RNA sequencing databases were downloaded from https://www.ncbi.nlm.nih.gov/. For scRNA-seq analysis, we employed standard clustering algorithms based on gene expression similarity. For the parameter settings, we used a resolution of 0.6, which helps achieve finer cell cluster separation while ensuring the accuracy and consistency of the tumor cell clusters. The cells annotation markers can be found in the referenced literature [24]. GESA analysis was performed using GSEA 4.3.3 software. Statistical analysis was performed using GraphPad Prism 9, with results presented as mean ± standard deviation (SD). For comparisons between two groups, an unpaired t-test was applied for normally distributed data, while the Mann-Whitney U test was used for non-normally distributed data. A p-value below 0.05 was considered statistically significant, with levels of significance denoted as: $p < 0.05$ (*), $p < 0.01$ (**), $p < 0.001$ (***), and $p < 0.0001$ (****).

Results

Prkci might function as a pro-metastatic factor

In order to investigate the role of Prkci in colorectal cancer and its potential involvement in metastasis, we firstly analyzed single-cell RNA sequencing of GSE110009 dataset, in which contained colon primary and liver metastasis tumor [24]. t-SNE plots from single-cell RNA sequencing data demonstrated the distribution of various cell types within the tumor microenvironment (Fig. 1A). We used the markers CDH1, EPCAM and CEACAM6 to identify tumor cells (Figure S1A). Cell distribution in the primary and metastases was shown in Fig. 1B. Next, we compared the gene expression of cancer cells from primary and liver metastasis. Interestingly, Prkci was significantly upregulated in liver metastasis cancer cells (Fig. 1C and Figure S1B). Considering that Prkci has been

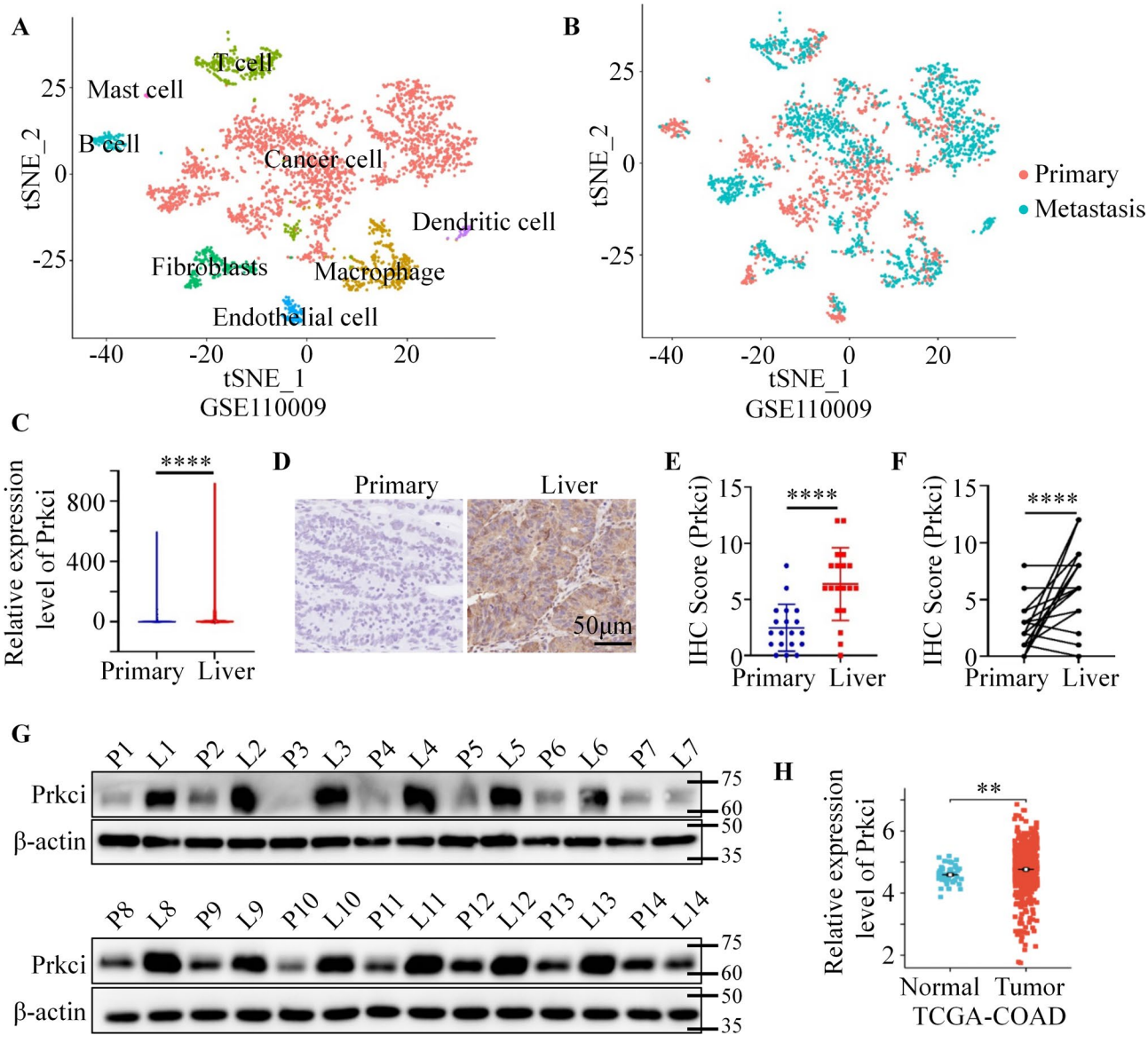

Fig. 1 Prkci was significantly upregulated in metastatic colorectal cancer tissues compared to primary tumors. (**A**) t-SNE plot from GSE110009 dataset showed the distribution of different cell types, including cancer cells, fibroblasts, and immune cells in colorectal primary and liver metastatic cancer samples. (**B**) t-SNE plot highlighted the segregation of primary tumor cells (red) and metastatic tumor cells (blue). (**C**) The violin plot showed the expression levels of Prkci in primary tumors and liver metastases. (**D**) 19 pairs of colorectal primary and liver metastasis tumor samples were collected for IHC assays. Representative IHC images showed Prkci staining in primary and liver metastatic tissues. (**E-F**) The scatter plot showed the IHC scores of Prkci in primary tumors and metastases. (**G**) 14 pairs of colorectal primary and liver metastasis tumor samples were collected for western blot assays. Western blot analysis showed the expression level of Prkci in liver metastatic tissues (**L**) and paired primary tissues (**P**). (**H**) The scatter plot showed the expression levels of Prkci in tumor tissues and normal tissues in the TCGA-COAD (Colon Adenocarcinoma) dataset. Each western blot assay was performed in triplicate, yielding consistent results. Statistical analysis was conducted using Student's t-test

established as an oncogene in osteosarcoma, pancreatic cancer, and cervical cancer, with limited studies addressing its role in colorectal cancer (CRC) metastasis, we further aimed to elucidate the functional implications of Prkci in CRC progression and metastatic potential. We then collected 19 pairs of colorectal primary and liver metastasis tumor samples. IHC analysis revealed a significant upregulation of Prkci in liver metastatic tissues compared to primary tumor tissues (Fig. 1D-F). Western blot analysis of 14 paired primary and liver metastatic tissues further validated that Prkci expression was higher in liver metastatic samples compared to their matched primary counterparts (Fig. 1G). This upregulation was further confirmed by TNMplot database, which showed stronger Prkci staining in liver metastatic samples compared to primary tumors (Figure S2A) [25]. We next compared Prkci levels in tumor versus normal tissues using TCGA database. Tumor tissues displayed a significantly elevated expression of Prkci compared to normal tissues (Fig. 1H), reinforcing the potential oncogenic role of Prkci in CRC. Consistently, Prkci was also upregulated in other kinds of tumor compared normal tissues (Figure S2B). Kaplan-Meier analysis revealed that patients with high Prkci expression had significantly reduced overall survival (OS) compared to those with low expression (Figure S2C). These results collectively suggested that Prkci was upregulated in CRC, particularly in metastatic lesions, implying its possible role as a pro-metastatic factor in colorectal cancer.

Prkci positively promoted migration and invasion in colorectal cancer cells

To further understand the functional role of Prkci in promoting colorectal cancer cell metastasis, we firstly conducted gain-of-function studies by overexpressing Prkci in SW48 and LoVo cell lines. Western blot analysis confirmed successful overexpression of HA-tagged Prkci in SW48 and LoVo cells (Fig. 2A). Trans-well assays were performed to analyze the migration and invasion ability of colorectal cancer cell ectopically expressing Vector or Prkci. Results indicated that Prkci overexpression significantly enhanced both migratory and invasive capacities of SW48 and LoVo cells compared to vector controls (Fig. 2B and C). Wound healing assay confirmed that Prkci-overexpressing cells demonstrated a faster closure of the wound gap in both SW48 and LoVo cell lines, indicating enhanced migratory abilities (Fig. 2D and E). Given the observed increase in migratory and invasive behaviors, we next examined whether Prkci overexpression induced epithelial-to-mesenchymal transition (EMT), a critical process in cancer metastasis. Western blot analysis showed that Prkci overexpression led to the downregulation of epithelial marker E-cadherin/ZO-1 and upregulation of mesenchymal markers N-cadherin/vimentin (Fig. 2F). Quantitative PCR analysis revealed that mRNA levels of EMT-related transcription factors, such as Snail, Vimentin and N-cadherin, were significantly increased in Prkci-overexpressing cells, while the expression of epithelial markers E-cadherin and ZO-1 was significantly decreased (Fig. 2G).

Subsequently, we performed loss-of-function experiments by knocking out Prkci in SW48 and LoVo cell lines. Western blotting confirmed Prkci knockout (Fig. 3A), and Trans-well assays showed significantly reduced migration and invasion in Prkci-knockout cells compared to controls (Fig. 3B and C). Prkci knockout impaired wound closure, indicating reduced migratory ability (Fig. 3D and E). Prkci knockout increased E-cadherin/ZO-1 and decreased N-cadherin/vimentin, suggesting EMT reversal (Fig. 3F and G). Furthermore, we re-expressed Prkci in Prkci knockout cells and found that Prkci re-expression could reverse the decreased cell migration and invasion abilities caused by PRKCI knockout using CRISPR-Cas9 technology (Figure S3A-C). In summary, Prkci positively significantly promoted migration and invasion and induced the mesenchymal-to-epithelial transition in colorectal cancer cells.

Prkci enhanced metastatic signaling via activation of the TGF-β pathway

To explore the detailed mechanism of Prkci-mediated tumor metastasis, we firstly conducted Gene Set Enrichment Analysis (GSEA) using multiple colorectal cancer GEO datasets. GSEA for single-cell RNA sequencing of Fig. 1A revealed that TGF-β signaling was enriched in metastatic samples compared to primary tumors (Fig. 4A). Meanwhile, GSEA performed on other multiple datasets showed a significant enrichment of TGF-β signaling in colorectal tumor samples with high Prkci expression (Figure S2A) [26–29]. These findings indicated a potential link between Prkci and TGF-β signaling in promoting metastasis. Western blot further demonstrated that Prkci positively promoted activation of the TGF-β pathway (Fig. 4B and figure S2B). Interestingly, Prkci could positively regulate the expression of Tgfbr1, a key receptor and initiator of the TGF-β signaling pathway. To validate whether Tgfbr1 was essential for Prkci-mediated TGF-β signaling pathway activation, we treated Prkci cells with PF-06952229, a TGF-β receptor inhibitor. PF-06952229 application reduced Smad2 and Smad3 phosphorylation in Prkci cells (Figure S2C). Also, knockdown of Tgfbr1 in Prkci cells reduced Smad2 phosphorylation, suggesting that Prkci required Tgfbr1 to activate TGF-β signaling (Fig. 4C). Meanwhile, Prkci re-expression could reverse the decreased TGF-β pathway activation caused by PRKCI knockout using CRISPR-Cas9 technology (Figure S4D). Next, we investigated how Prkci regulated Tgfbr1 expression. We

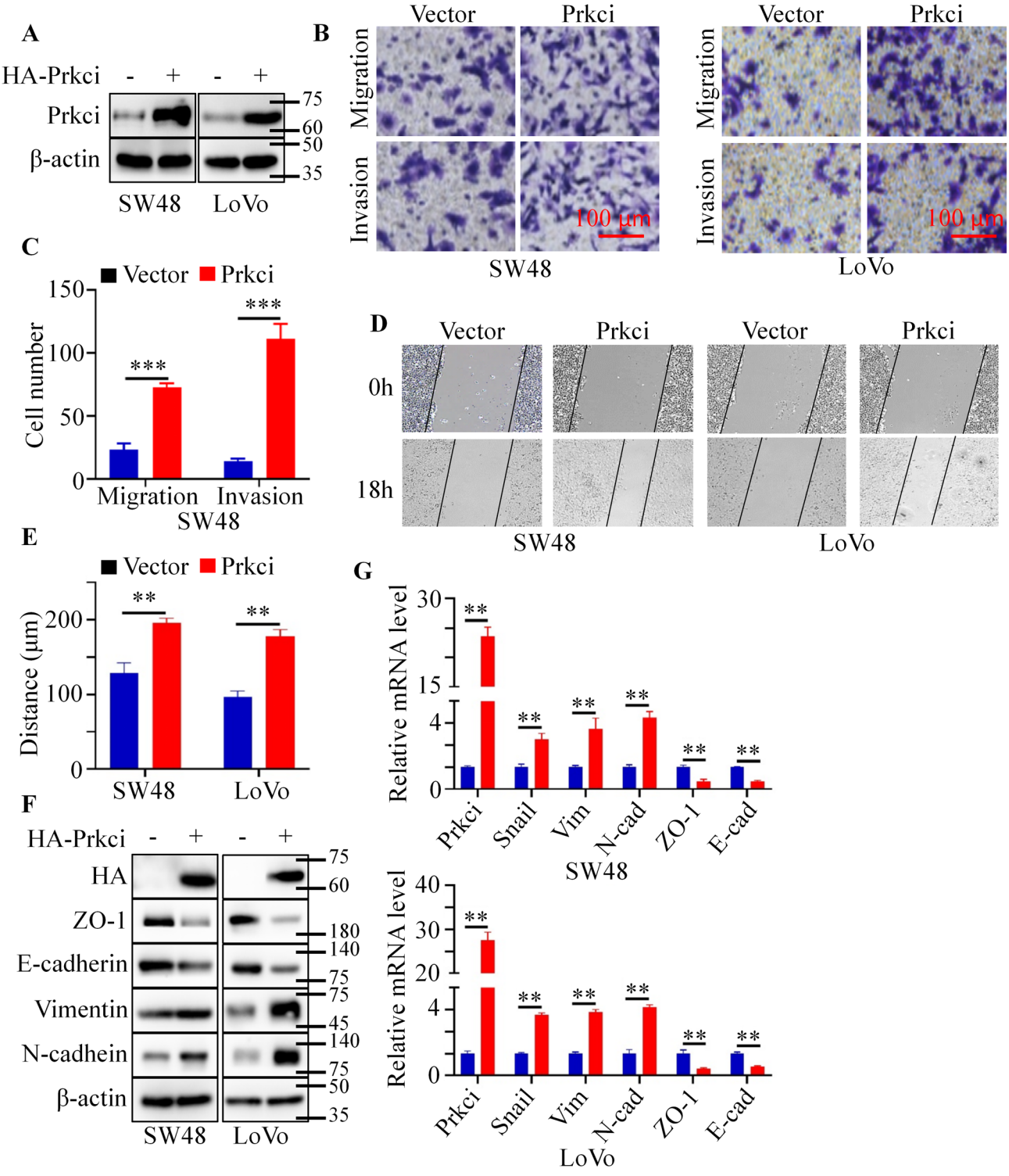

Fig. 2 Overexpression of Prkci promoted migration, invasion, and EMT in colorectal cancer cells. (**A**) Western blot analysis showed the expression level of Prkci in designated cell lines. (**B**) The representative results of Trans-well assays using designated cell lines. (**C**) Quantification of Trans-well assay results from Fig. 2B. (**D**) The representative results of Wound healing assays using designated cell lines. (**E**) Quantitative analysis of wound healing assays from Fig. 2D. (**F**) Western blot analysis showed the expression level of target proteins in designated cell lines. (**G**) Quantitative RT-PCR analysis showed the expression level of target mRNAs in designated cell lines. Each western blot assay was performed in triplicate, yielding consistent results. Statistical analysis was conducted using Student's t-test

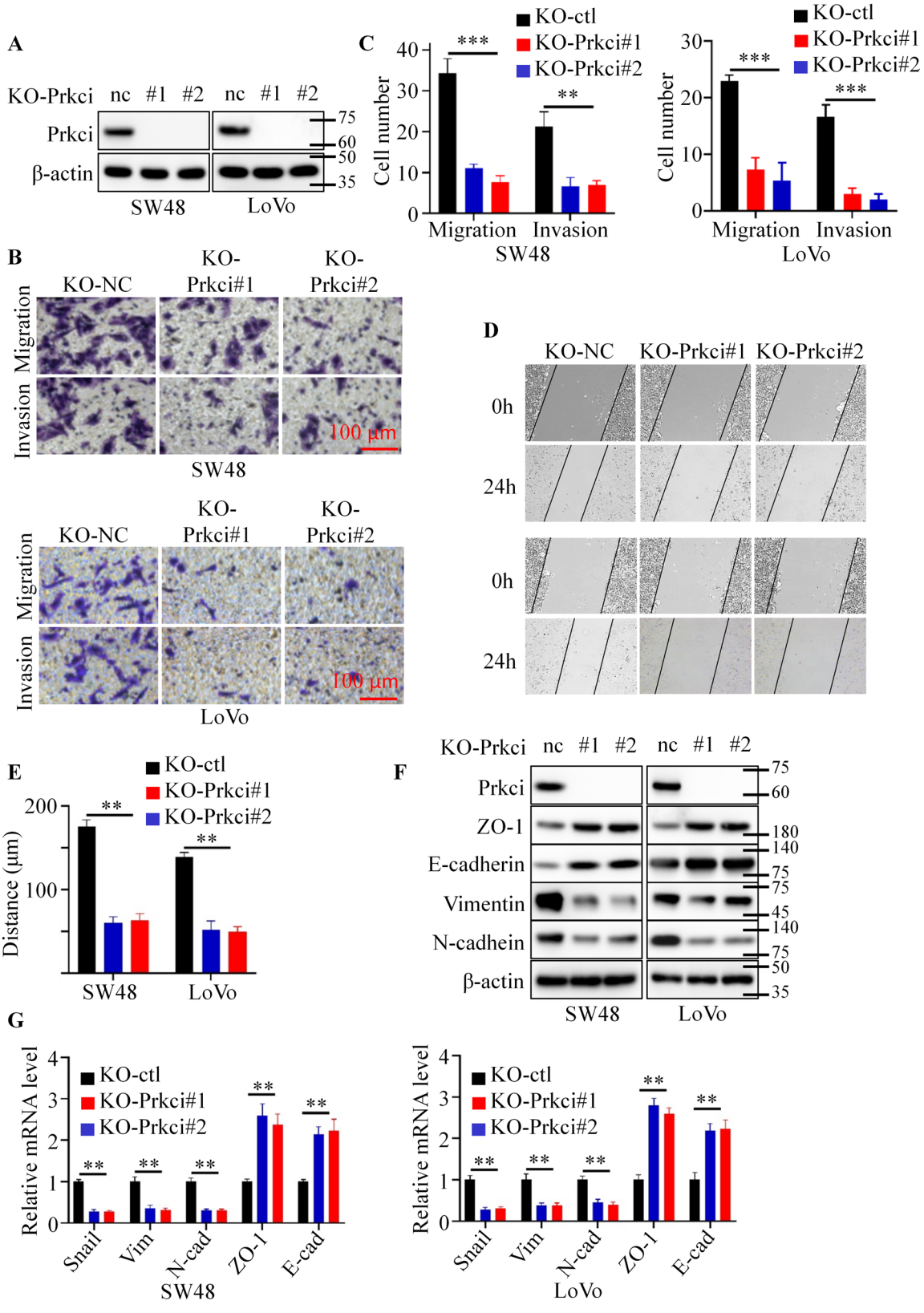

Fig. 3 (See legend on next page.)

(See figure on previous page.)

Fig. 3 Knockout of Prkci inhibited migration, invasion, and EMT in colorectal cancer cells. (**A**) Western blot analysis showed the expression level of Prkci in designated cell lines. (**B**) The representative results of Trans-well assays using designated cell lines. (**C**) Quantification of Trans-well assay results from Fig. 3B. (**D**) The representative results of Wound healing assays using designated cell lines. (**E**) Quantitative analysis of wound healing assays from Fig. 3D. (**F**) Western blot analysis showed the expression level of target proteins in designated cell lines. (**G**) Quantitative RT-PCR analysis showed the expression level of target mRNAs in designated cell lines. Each western blot assay was performed in triplicate, yielding consistent results. Statistical analysis was conducted using Student's t-test. Each western blot assay was performed in triplicate, yielding consistent results. Statistical analysis was conducted using Student's t-test

firstly detected the mRNA level of Tgfbr1 after interfering with Prkci expression. RT-PCR analysis revealed that Prkci overexpression or knockout did not alter the mRNA levels of Tgfbr1, suggesting that Prkci regulated Tgfbr1 post-transcriptionally (Figure S5A). Considering that lysosomes and proteasomes were the two most main pathways for protein degradation, we used MG132, a proteasome inhibitor, or chloroquine (CQ), a lysosome inhibitor, to treat KO-NC and KO-Prkci cells. MG132 abrogated Prkci knockout-mediated Tgfbr1 expression repression, while chloroquine (CQ) treatment had no this effect, suggesting Prkci stabilizes Tgfbr1 by preventing its proteasomal degradation (Fig. 4D). Next, we transfected his-ubiquitin plasmid into identified SW48 cells and MG132 was applied to inhibit the degradation of endogenous Tgfbr1. Immunoprecipitation and Western blotting assays were conducted to detect the poly-ubiquitin level of Tgfbr1. Results showed that Prkci overexpression significantly inhibited the poly-ubiquitin level of Tgfbr1, while Prkci knockout obviously upregulated the poly-ubiquitin level of Tgfbr1 (Fig. 4E and F). Next, we explored the specific type of ubiquitin linkage through which Prkci regulates Tgfbr1. To this end, we created a series of ubiquitin mutants, mutating one lysine (K) to arginine (R) while keeping the other lysine residues unchanged. Immunoprecipitation and Western blotting assays showed that only K11R mutant ubiquitin could abolish Prkci-mediated Tgfbr1 ubiquitination (Fig. 4G and Figure S5B). Also, we used anti-ubiquitin K11 linkage antibody to detect K11 ubiquitin chains, and results showed that Prkci can regulate the K11-linked ubiquitination of Tgfbr1 (Fig. 4H). Collectively, Prkci positively regulated TGF-β signaling via inhibiting the K11-linked ubiquitin of Tgfbr1.

Prkci stabilized and enhanced phosphorylation of Tgfbr1

To further investigate how Prkci regulated Tgfbr1 expression, we firstly conducted co-immunoprecipitation assays. Results showed that there was a physical interaction between Prkci and Tgfbr1 (Fig. 5A). Considering that Prkci was a serine/ threonine-protein kinase, we assumed that Prkci might phosphorylated Tgfbr1. Of note, we also observed an increase in the phosphorylation of Tgfbr1 in cells overexpressing Prkci, while the phosphorylation level of Tgfbr1 was reduced in Prkci-knockout cells (Fig. 5B and C). To determine the region of Tgfbr1 responsible for interaction with Prkci, we constructed two segmented plasmids according to the GS domain and kinase domain (Fig. 5D). Co-IP assays confirmed that Prkci interacted with the 1-174 aa of Tgfbr1 (Fig. 5E and figure S5C). After browsing the PhosphoSitePlus database, we found that there were four potential phosphorylation of serine/ threonine. We individually replaced these amino acids with alanine (A) to mimic phosphorylation-deficient mutations. Western blots revealed that the T47A mutation disrupted Prkci-mediated phosphorylation of Tgfbr1. This indicated that Prkci phosphorylated Tgfbr1 at threonine 47 (Fig. 5F). Sequence alignment analysis across species demonstrated that the Tgfbr1 phosphorylation site (highlighted in red) was conserved, suggesting an evolutionary importance in TGF-β signaling (Fig. 5G).

Subsequently, we detected the functional impact of T47 phosphorylation sites on Tgfbr1. We firstly constructed SW48 cells stably separately expressing Tgfbr1 T47A, Tgfbr1 WT, and T47E (phosphorylation-mimetic) mutant using Tgfbr1 knock-out cell (Figure S5D, S5E). Western blot analysis revealed that Tgfbr1 T47A had higher poly-ubiquitin level than Tgfbr1 WT, while Tgfbr1 T47E had lower poly-ubiquitin level than Tgfbr1 WT, suggesting Tgfbr1 T47 phosphorylation blocked its poly-ubiquitin (Fig. 5H). Meanwhile, Cells expressing Tgfbr1 T47A mutation showed reduced levels of phosphorylated Smad2 compared to wild-type cells. Additionally, T47A cells had decreased expression of mesenchymal markers and increased expression of the epithelial markers, while the T47E mutation enhanced mesenchymal markers and reduced E-cadherin levels, suggesting that T47 phosphorylation promoted EMT (Fig. 5I and J). Transwell assays revealed that the T47A mutation significantly reduced migration and invasion compared to WT, while the T47E mutation enhanced these abilities, aligning with the effects of these mutations on EMT marker expression (Fig. 5K and L). In summary, these results showed that Prkci interacted with Tgfbr1, enhanced its phosphorylation at T47, and T47 phosphorylation of Tgfbr1 was critical for promoting EMT and enhancing migration and invasion in colorectal cancer cells.

Tgfbr1 T47 phosphorylation was an essential thing for Prkci-mediated TGF-β pathway activation

To further reveal the relationship between Prkci and TGF-β pathway, we firstly constructed SW48 cell lines stably expressing Vector + Tgfbr1 WT, Prkci + Tgfbr1

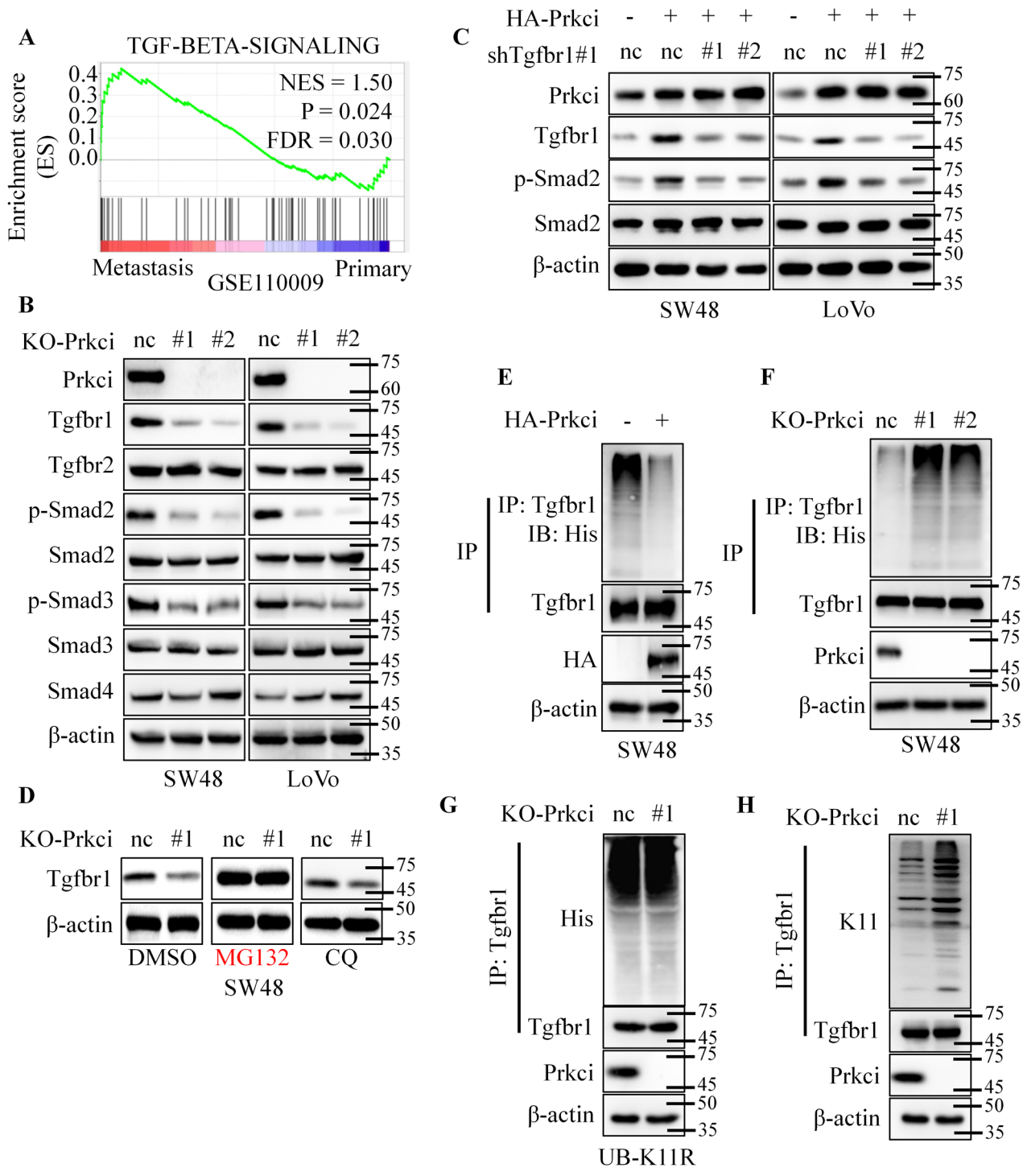

Fig. 4 Prkci promoted metastatic signaling by activating the TGF-β pathway. (**A**) Gene Set Enrichment Analysis (GSEA) of single-cell RNA sequencing data revealed enrichment of TGF-β signaling in metastatic colorectal cancer samples compared to primary tumors. (**B**, **C**) Western blot analysis showed the expression level of target proteins in the designated cell lines. (**D**) MG132 and CQ were applied to treat the designated cell lines. Western blot showed the expression level of target proteins. (**E**, **F**) His-ubiquitin plasmids were transfected into the designated cell lines. MG132 was used to the degradation of endogenous Tgfbr1. Immunoprecipitation and Western blotting assays showed the ploy-ubiquitination level of Tgfbr1. (**G**) SW48 cells were transfected with K11R His-ubiquitin plasmids. IP and IB analysis to show the poly-ubiquitination of Tgfbr1 in KO-NC or KO-Prkci cells. (**H**) IP and IB analysis to show the K11-polyubiquitination of Tgfbr1 in KO-NC or KO-Prkci cells using anti-ubiquitin K11 linkage antibody. Each western blot assay was performed in triplicate, yielding consistent results. Each western blot assay was performed in triplicate, yielding consistent results

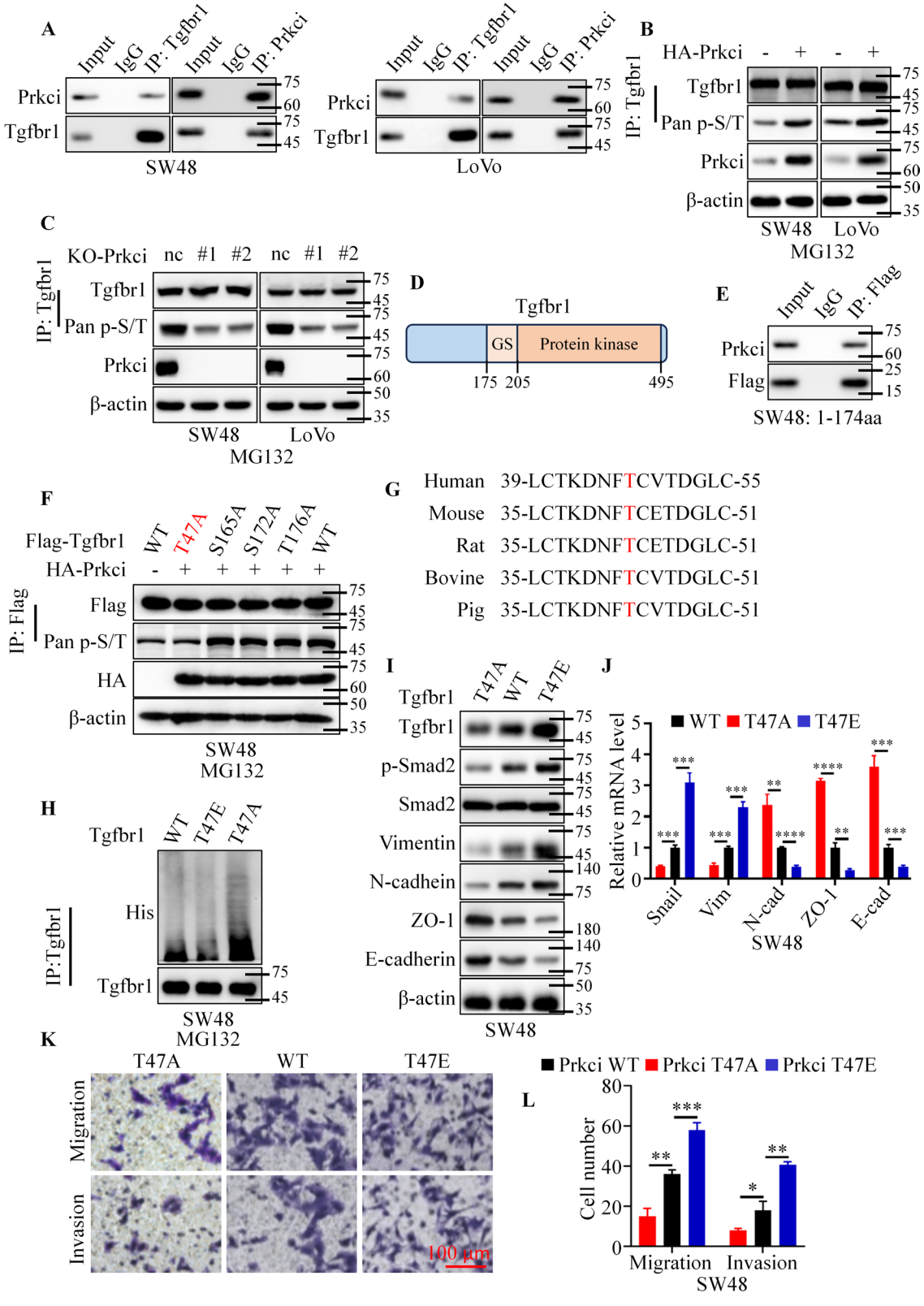

Fig. 5 (See legend on next page.)

(See figure on previous page.)

Fig. 5 Prkci phosphorylated Tgfbr1 at threonine 47, promoting EMT and enhancing migration and invasion in colorectal cancer cells. (**A**) Co-immunoprecipitation (Co-IP) assays revealed a physical interaction between Prkci and Tgfbr1 in SW48 and LoVo cell lines. (**B**, **C**) Immunoprecipitation and western blot analysis showed the phosphorylation level of serine/threonine residues on Tgfbr1 in the designated cell lines. (**D**) Schematic representation of Tgfbr1 domains. (**E**) Co-IP confirmed the interaction between Prkci and the 1–174 region of Tgfbr1. (**F**) HA-Prkci and Flag-Tgfbr1 mutants were transfected into SW48 cells separately, Immunoprecipitation and western blot analysis showed the phosphorylation level of serine/threonine residues on Tgfbr1. (**G**) Sequence alignment across species revealed that the T47 site was evolutionarily conserved. (**H**) His-ubiquitin plasmids were transfected into the designated cell lines. MG132 was used to the degradation of Tgfbr1. Immunoprecipitation and western blot analysis showed the ploy-ubiquitination level of Tgfbr1 in Tgfbr1 WT, T47A and T47E cells. (**I**, **J**) Western blot and RT-PCR analysis showed the expression level of target proteins/mRNAs. (**K**) The representative results of Trans-well assays using designated cell lines. (**L**) Quantification of Trans-well assay results from Fig. 5K. Each western blot assay was performed in triplicate, yielding consistent results. Statistical analysis was conducted using Student's t-test

WT or Prkci + Tgfbr1 T47A. Western blotting assays showed that Prkci overexpression significantly activated TGF-β pathway, decreased epithelial markers, and increased mesenchymal markers in Tgfbr1 WT cells, but not Tgfbr1 T47A cells (Fig. 6A and B). Also, Trans-well assays revealed that the Prkci overexpression obviously promoted migration and invasion in Tgfbr1 WT cells, but not Tgfbr1 T47A cells (Fig. 6C and D). Next, we generated SW48 cell lines stably expressing KO-NC + Vector, KO-Prkci + Vector or KO-Prkci + Tgfbr1 T47E. Western blotting assays demonstrated that Prkci knock-out markedly inhibited the activation of the TGF-β pathway, upregulated epithelial markers, and downregulated mesenchymal markers in Tgfbr1 WT cells, whereas these effects were not observed in Tgfbr1 T47E cells (Fig. 6E and F). Additionally, Transwell assays indicated that Prkci knock-out significantly abrogated migration and invasion in Tgfbr1 WT cells but had no such effect in Tgfbr1 T47E cells (Fig. 6G and H). Collectively, our results revealed that Prkci-mediated TGF-β pathway activation relied on Tgfbr1 T47 phosphorylation.

Targeting Prkci significantly inhibited colorectal cancer metastasis in vivo

To evaluate the effect of Prkci on metastasis and survival in vivo, we utilized a mouse model with Prkci knockout SW48 cancer cells. For the lung metastasis model, cancer cells were injected into the tail vein, allowing them to circulate and colonize in the lungs [30]. After 2 months, all mice were sacrificed, and lungs were isolated. Representative images of lung tissues collected from the KO-ctl, KO-Prkci#1, and KO-Prkci#2 groups showed visible metastatic nodules (Fig. 7A). Quantification of lung metastatic nodules revealed a significant reduction in both KO-Prkci#1 and KO-Prkci#2 groups compared to the KO-ctl group (Fig. 7B). Additionally, the lung weights of KO-Prkci mice were significantly lower than those of controls, indicating a reduced metastatic burden in the lungs (Fig. 7C). Survival analysis was conducted to assess the impact of Prkci knockout on lifespan in the context of lung metastasis. Kaplan-Meier survival curves showed that KO-Prkci mice had a significantly prolonged survival compared to KO-ctl mice, with both KO-Prkci#1 and KO-Prkci#2 groups exhibiting extended survival times (Fig. 7D).

In the liver metastasis model, cancer cells were injected into the spleen to enable liver colonization [30]. After 2 months, all mice were sacrificed and the mice livers were isolated and subjected to bioluminescent imaging, with representative results shown in Fig. 7F. Quantitative analysis confirmed significantly lower bioluminescent signaling in KO-Prkci#1 and KO-Prkci#2 groups compared to KO-ctl, which mean that Prkci knock-out significantly inhibited colorectal cancer liver metastasis (Fig. 7G). Liver weights further corroborated the reduced tumor burden in KO-Prkci mice (Fig. 7H). Kaplan-Meier survival curves for the liver metastasis model demonstrated significantly prolonged survival in the KO-Prkci groups compared to controls (Fig. 7I). Immunohistochemical analysis of lung and liver tissues revealed decreased expression of Prkci, Tgfbr1, and p-Smad3 in KO-Prkci#1 and KO-Prkci#2 groups compared to KO-ctl (Fig. 7E, J). These findings indicated that Prkci played a critical role in promoting lung and liver metastasis and activating the TGF-β/Smad3 pathway in vivo.

Discussion

The findings presented in this study establish a novel oncogenic role for Prkci in colorectal cancer (CRC) metastasis. Our results demonstrate that Prkci is significantly upregulated in metastatic CRC tissues compared to primary tumors and normal tissues. Mechanistically, Prkci promotes metastasis by phosphorylating and stabilizing Tgfbr1, thereby amplifying the TGF-β signaling cascade that drives epithelial-to-mesenchymal transition (EMT), tumor cell invasion, and dissemination. Importantly, we identified threonine 47 (T47) as a critical phosphorylation site on Tgfbr1 mediated by Prkci. This phosphorylation event stabilizes Tgfbr1 by reducing its polyubiquitination and subsequent proteasomal degradation. In vivo models further validated the critical role of Prkci in CRC metastasis. Knockout of Prkci in CRC cells significantly reduced liver and lung metastasis and improved survival outcomes in mice, highlighting its potential as a therapeutic target.

Previous studies have highlighted the role of Prkci as an oncogene in various cancers through activating critical

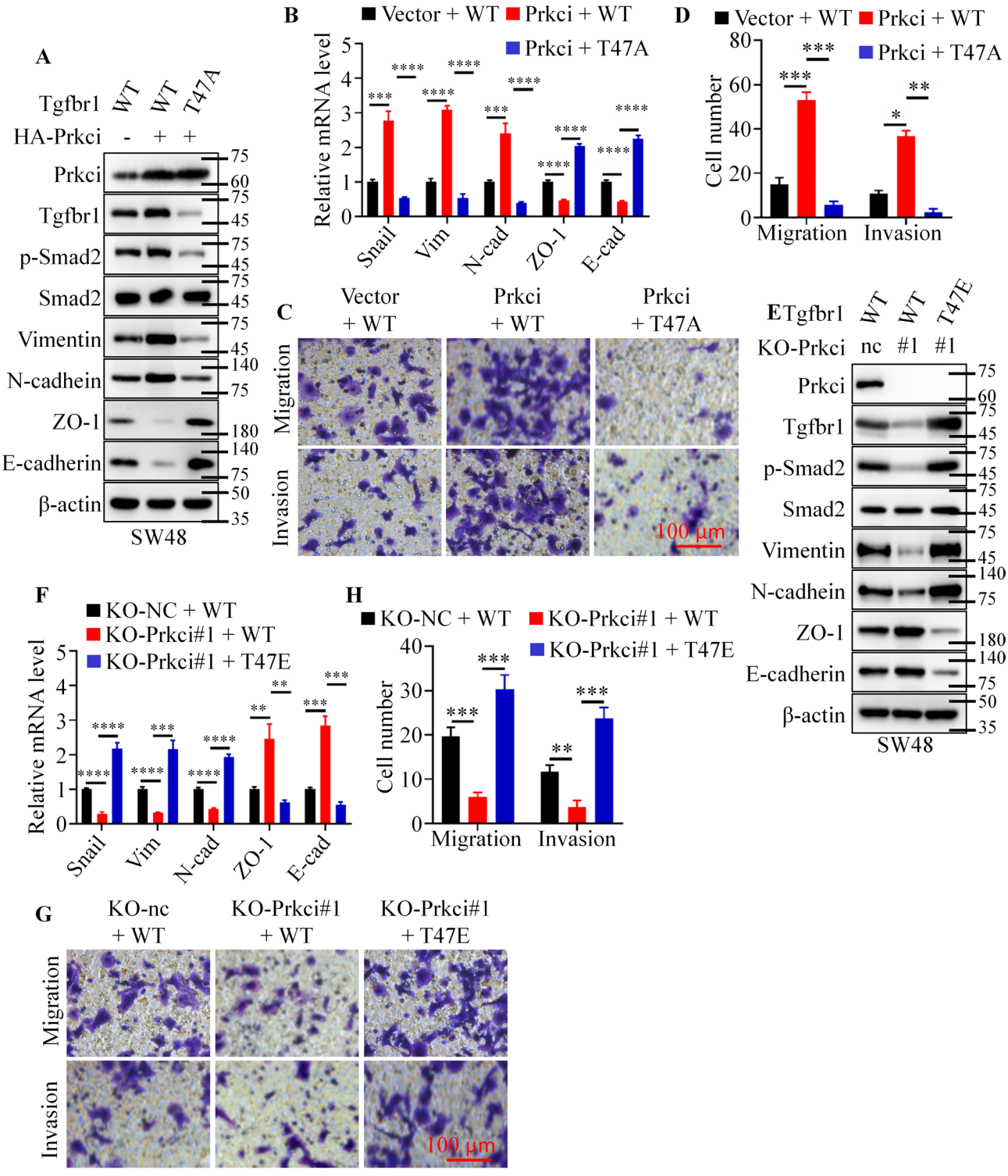

Fig. 6 Prkci promoted migration, invasion, and EMT through Tgfbr1 phosphorylation at threonine 47. (**A**, **B**, **E**, **F**) Western blot and RT-PCR analysis showed the expression level of target proteins/mRNAs. (**C**, **G**) The representative results of Trans-well assays using designated cell lines. (**D**, **H**) Quantification of Trans-well assay results from Fig. 6C/6G. Each western blot assay was performed in triplicate, yielding consistent results. Statistical analysis was conducted using Student's t-test

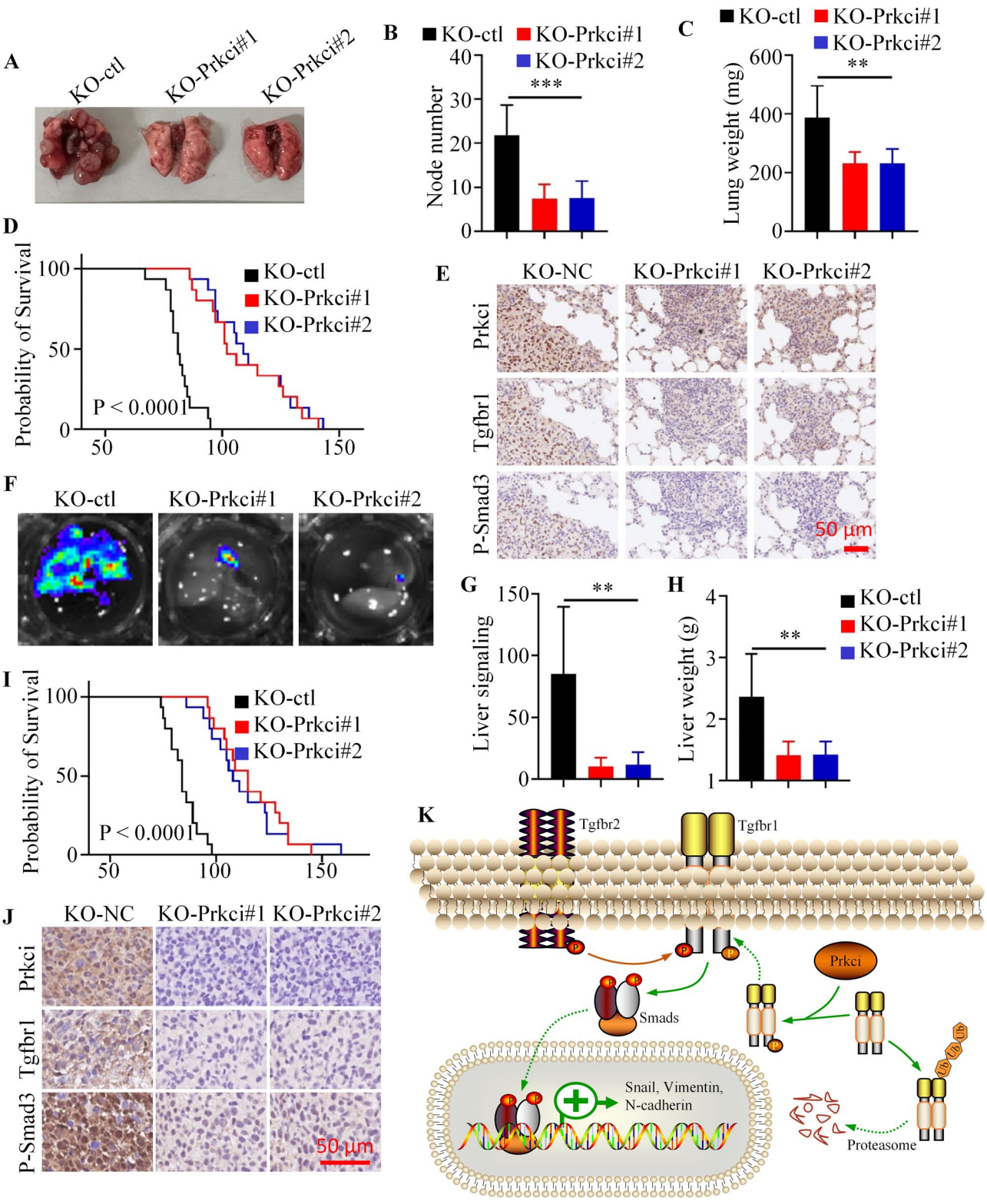

Fig. 7 (See legend on next page.)

(See figure on previous page.)

Fig. 7 Targeting Prkci suppressed lung and liver metastases and improved survival in vivo. (**A**) Representative images of lungs from mice injected with Prkci-knockout or control colorectal cancer cells. (**B**, **C**) Quantification of lung metastatic nodules and lung weights ($n=8$). (**D**) Kaplan-Meier survival curves showed the survival time of these three groups lung metastases mice ($n=15$). (**E**) Immunohistochemical analysis of lung tissues revealed the expression of Prkci, Tgfbr1, and P-Smad3 in of these three groups mice lung metastases. (**F**) Representative bioluminescent images of liver metastases. (**G**, **H**) Quantification of liver metastatic signals and liver weights ($n=8$). (**I**) Kaplan-Meier survival curves showed the survival time of these three groups liver metastases mice ($n=15$). (**J**) Immunohistochemical analysis of lung tissues revealed the expression of Prkci, Tgfbr1, and P-Smad3 in of these three groups mice liver metastases. (**K**) Schematic diagram illustrated the proposed mechanism by which Prkci phosphorylated and stabilized Tgfbr1, promoting TGF-β/Smad3 signaling, epithelial-to-mesenchymal transition, and metastasis. Statistical analysis was conducted using Student's t-test

oncogenic pathways such as YAP, PI3K/ATK, NFKB and P53 signaling [12, 13, 15, 19, 22]. However, in our study, we revealed that PRKCI can regulate tumor metastasis in colorectal cancer by modulating the TGFB1 signaling pathway, further complementing previous research findings. Additionally, it is noteworthy that in a study on alveolar rhabdomyosarcoma, the authors used aurothiomalate (ATM) to inhibit Prkci activity and demonstrated promising therapeutic effects [31]. This suggests a potential clinical strategy for targeted intervention in tumor metastasis.

The TGF-β signaling pathway is a well-established driver of EMT, facilitating the loss of epithelial markers such as E-cadherin and the gain of mesenchymal traits like N-cadherin and vimentin [6, 7, 11, 32]. Our results show that Prkci overexpression in CRC cells enhances EMT, while its inhibition reverses EMT, as evidenced by changes in marker expression and migratory/invasive behaviors. Our study provides a foundation for developing targeted therapies aimed at disrupting the Prkci-Tgfbr1 axis. Such therapies could be used in combination with existing treatment modalities, including immune checkpoint inhibitors and chemotherapies, to improve outcomes in CRC patients. Although Tgfb-targeting monoclonal antibodies have shown promising results in some clinical trials, they remain controversial [33, 34]. The Prkci-Tgfbr1 signaling axis proposed in this study may provide an alternative approach for intervening in the TGFB1 signaling pathway.

Despite these promising findings, there are limitations to our study. First, the precise upstream regulators of Prkci in CRC remain to be identified. Second, the potential off-target effects of Prkci inhibition require further investigation to ensure clinical safety. Lastly, the applicability of our findings to human patients needs validation through clinical studies and patient-derived models.

In conclusion, our study uncovers a critical role for Prkci in CRC metastasis by stabilizing and activating Tgfbr1, leading to enhanced TGF-β signaling and EMT. Targeting Prkci could provide a novel and effective strategy for mitigating CRC metastasis and improving patient survival.

Supplementary Information

The online version contains supplementary material available at https://doi.org/10.1186/s12964-025-02236-6.

Supplementary Material 1

Supplementary Material 2

Supplementary Material 3

Supplementary Material 4

Supplementary Material 5

Supplementary Material 6

Acknowledgements
Not applicable.

Author contributions
Peng Li: Conceptualized the study, performed data analysis and interpretation, provided critical feedback, drafted the manuscript and approved the final version of the manuscript. Guangshi Liu: Conducted experiments and contributed to data analysis. Wenbin Zhang: Participated in study design, data interpretation, and manuscript revisions. Tao Li: Supervised the study.

Funding
This work was funded by the Xinjiang Uygur Autonomous Region Tianshan Talent Training Program (2023TSYCCX0060), the Natural Science Foundation of Xinjiang Uygur Autonomous Region (2022D01D77), and the Tianshan Talent Training Program (TSYC202301A031).

Data availability
No datasets were generated or analysed during the current study.

Declarations

Ethics approval and consent to participate
This study was approved by the Ethical Committee of the People's Hospital of Xinjiang Uygur Autonomous Region, and all participants provided written informed consent. Animal experiments were conducted following protocols approved by the Institutional Animal Care and Use Committee at the same institution.

Consent for publication
All authors have reviewed and consented to the publication of this manuscript.

Competing interests
The authors declare no competing interests.

Received: 17 December 2024 / Accepted: 9 May 2025
Published online: 17 May 2025

References

1. Mi M, Weng S, Xu Z, Hu H, Wang Y, Yuan Y. CSCO guidelines for colorectal cancer version 2023: updates and insights. Chin J Cancer Res. 2023;35(3):233–8.
2. Puccini A, Lenz HJ. Colorectal cancer in 2017: Practice-changing updates in the adjuvant and metastatic setting. Nat Rev Clin Oncol. 2018;15(2):77–8.
3. Tsilimigras DI, Brodt P, Clavien PA, Muschel RJ, D'Angelica MI, Endo I, et al. Liver metastases. Nat Rev Dis Primers. 2021;7(1):27.

4. Di Nicolantonio F, Vitiello PP, Marsoni S, Siena S, Tabernero J, Trusolino L, et al. Precision oncology in metastatic colorectal cancer - from biology to medicine. Nat Rev Clin Oncol. 2021;18(8):506–25.
5. Wang X, Eichhorn PJA, Thiery JP. TGF-beta, EMT, and resistance to anti-cancer treatment. Semin Cancer Biol. 2023;97:1–11.
6. Zhang YE, Stuelten CH. Alternative splicing in EMT and TGF-beta signaling during cancer progression. Semin Cancer Biol. 2024;101:1–11.
7. Padua D, Massague J. Roles of TGFbeta in metastasis. Cell Res. 2009;19(1):89–102.
8. Marvin DL, Heijboer R, Ten Dijke P, Ritsma L. TGF-beta signaling in liver metastasis. Clin Transl Med. 2020;10(7):e160.
9. Gough NR, Xiang X, Mishra L. TGF-beta signaling in liver, pancreas, and Gastrointestinal diseases and Cancer. Gastroenterology. 2021;161(2):434–52. e15.
10. Derynck R, Turley SJ, Akhurst RJ. TGFbeta biology in cancer progression and immunotherapy. Nat Rev Clin Oncol. 2021;18(1):9–34.
11. Jung B, Staudacher JJ, Beauchamp D. Transforming growth factor beta superfamily signaling in development of colorectal Cancer. Gastroenterology. 2017;152(1):36–52.
12. Qu L, Xin Y, Feng J, Ren X, Li Z, Chen X, et al. Downregulation of PRKCI inhibits osteosarcoma cell growth by inactivating the Akt/mTOR signaling pathway. Front Oncol. 2024;14:1389136.
13. Jiao J, Ruan L, Cheng CS, Wang F, Yang P, Chen Z. Paired protein kinases PRKCI-RIPK2 promote pancreatic cancer growth and metastasis via enhancing NF-kappaB/JNK/ERK phosphorylation. Mol Med. 2023;29(1):47.
14. Wu Z, Huang C, Li R, Li H, Lu H, Lin Z. PRKCI mediates radiosensitivity via the Hedgehog/GLI1 pathway in cervical Cancer. Front Oncol. 2022;12:887139.
15. Wang Y, Justilien V, Brennan KI, Jamieson L, Murray NR, Fields AP. PKCiota regulates nuclear YAP1 localization and ovarian cancer tumorigenesis. Oncogene. 2017;36(4):534–45.
16. Rehmani H, Li Y, Li T, Padia R, Calbay O, Jin L, et al. Addiction to protein kinase ci due to PRKCI gene amplification can be exploited for an aptamer-based targeted therapy in ovarian cancer. Signal Transduct Target Ther. 2020;5(1):140.
17. Abdelatty A, Fang D, Wei G, Wu F, Zhang C, Xu H, et al. PKCiota is a promising prognosis biomarker and therapeutic target for pancreatic Cancer. Pathobiology. 2022;89(6):370–81.
18. Justilien V, Walsh MP, Ali SA, Thompson EA, Murray NR, Fields AP. The PRKCI and SOX2 oncogenes are coamplified and cooperate to activate Hedgehog signaling in lung squamous cell carcinoma. Cancer Cell. 2014;25(2):139–51.
19. Qu L, Li G, Xia D, Hongdu B, Xu C, Lin X, et al. PRKCI negatively regulates autophagy via PIK3CA/AKT-MTOR signaling. Biochem Biophys Res Commun. 2016;470(2):306–12.
20. Sarkar S, Bristow CA, Dey P, Rai K, Perets R, Ramirez-Cardenas A, et al. PRKCI promotes immune suppression in ovarian cancer. Genes Dev. 2017;31(11):1109–21.
21. Inman KS, Liu Y, Scotti Buzhardt ML, Leitges M, Krishna M, Crawford HC et al. Prkci regulates autophagy and pancreatic tumorigenesis in mice. Cancers (Basel). 2022;14(3).
22. Yin N, Liu Y, Khoor A, Wang X, Thompson EA, Leitges M, et al. Protein kinase Ciota and Wnt/beta-Catenin signaling: alternative pathways to Kras/Trp53-Driven lung adenocarcinoma. Cancer Cell. 2019;36(2):156–67. e7.
23. Yin N, Liu Y, Khoor A, Wang X, Thompson EA, Leitges M, et al. Protein kinase Ciota and Wnt/beta-Catenin signaling: alternative pathways to Kras/Trp53-Driven lung adenocarcinoma. Cancer Cell. 2019;36(6):692–3.
24. Wang R, Li J, Zhou X, Mao Y, Wang W, Gao S, et al. Single-cell genomic and transcriptomic landscapes of primary and metastatic colorectal cancer tumors. Genome Med. 2022;14(1):93.
25. Bartha A, Gyorffy B. TNMplot.com: A web tool for the comparison of gene expression in normal, tumor and metastatic tissues. Int J Mol Sci. 2021;22(5).
26. Staub E, Groene J, Heinze M, Mennerich D, Roepcke S, Klaman I, et al. An expression module of WIPF1-coexpressed genes identifies patients with favorable prognosis in three tumor types. J Mol Med (Berl). 2009;87(6):633–44.
27. Ferrandon S, DeVecchio J, Duraes L, Chouhan H, Karagkounis G, Davenport J, et al. CoA synthase (COASY) mediates radiation resistance via PI3K signaling in rectal Cancer. Cancer Res. 2020;80(2):334–46.
28. Levine EA, Votanopoulos KI, Qasem SA, Philip J, Cummins KA, Chou JW, et al. Prognostic molecular subtypes of Low-Grade Cancer of the appendix. J Am Coll Surg. 2016;222(4):493–503.
29. Smith JJ, Deane NG, Wu F, Merchant NB, Zhang B, Jiang A, et al. Experimentally derived metastasis gene expression profile predicts recurrence and death in patients with colon cancer. Gastroenterology. 2010;138(3):958–68.
30. Gomez-Cuadrado L, Tracey N, Ma R, Qian B, Brunton VG. Mouse models of metastasis: progress and prospects. Dis Model Mech. 2017;10(9):1061–74.
31. Kikuchi K, Soundararajan A, Zarzabal LA, Weems CR, Nelon LD, Hampton ST, et al. Protein kinase C Iota as a therapeutic target in alveolar rhabdomyosarcoma. Oncogene. 2013;32(3):286–95.
32. Avolio M, Trusolino L. Rational treatment of metastatic colorectal cancer: A reverse Tale of men, mice, and culture dishes. Cancer Discov. 2021;11(7):1644–60.
33. Yen YT, Zhang Z, Chen A, Qiu Y, Liu Q, Wang Q, et al. Enzymatically responsive nanocarriers targeting PD-1 and TGF-beta pathways reverse immunotherapeutic resistance and elicit robust therapeutic efficacy. J Nanobiotechnol. 2025;23(1):124.
34. Oh DY, Ikeda M, Lee CK, Rojas C, Hsu CH, Kim JW, et al. Bintrafusp Alfa and chemotherapy as first-line treatment in biliary tract cancer: A randomized phase 2/3 trial. Hepatology. 2025;81(3):823–36.

Publisher's note